

# Computational parametric Willmore flow

Gerhard Dziuk

Received: 29 August 2007 / Revised: 22 July 2008  
© Springer-Verlag 2008

**Abstract** We propose a new algorithm for the computation of Willmore flow. This is the  $L^2$ -gradient flow for the Willmore functional, which is the classical bending energy of a surface. Willmore flow is described by a highly nonlinear system of PDEs of fourth order for the parametrization of the surface. The spatially discrete numerical scheme is stable and consistent. The discretization relies on an adequate calculation of the first variation of the Willmore functional together with a derivation of the second variation of the area functional which is well adapted to discretization techniques with finite elements. The algorithm uses finite elements on surfaces. We give numerical examples and tests for piecewise linear finite elements. A convergence proof for the full algorithm remains an open question.

**Mathematics Subject Classification (2000)** 35K55 · 65M15 · 65M60

## 1 Introduction

The purpose of this work is to derive a finite element method for the evolution of  $n$ -dimensional surfaces according to Willmore flow. Willmore flow is the  $L^2(\Gamma)$ -gradient flow of the Willmore functional

$$W(X) = \frac{1}{2} \int_{\Gamma} H^2, \quad (1.1)$$

---

G. Dziuk (✉)  
Abteilung für Angewandte Mathematik, Universität Freiburg,  
Hermann-Herder-Str. 10, 79104 Freiburg, Germany  
e-mail: gerd@mathematik.uni-freiburg.de

for a smooth, immersed, orientable, closed,  $n$ -dimensional surface  $\Gamma$ , which is parametrized locally by  $X : \Omega \rightarrow \Gamma$  in  $\mathbb{R}^{n+1}$  with parameter domain  $\Omega \subset \mathbb{R}^n$ . Here  $H = \kappa_1 + \dots + \kappa_n$  denotes the mean curvature of  $\Gamma$ . The first variation of (1.1) in the direction of  $\Phi : \Omega \rightarrow \mathbb{R}^{n+1}$  is given by

$$\begin{aligned} \langle W'(X), \Phi \rangle &= \left. \frac{d}{d\varepsilon} \right|_{\varepsilon=0} W(X + \varepsilon\Phi) \\ &= - \int_{\Gamma} \Phi \cdot \nu \left( \Delta_{\Gamma} H - \frac{1}{2} H^3 + H|\mathcal{H}|^2 \right), \end{aligned} \quad (1.2)$$

where  $\nu$  is the normal to  $\Gamma$  and  $\Delta_{\Gamma}$  is the Laplace–Beltrami-operator on  $\Gamma$ . The orientation is taken such that  $H$  is positive for spheres and the normal points away from the origin.  $|\mathcal{H}|^2 = \kappa_1^2 + \dots + \kappa_n^2$  is the square of the second fundamental form. For a derivation of this formula, see [21]. One part of this paper will be a derivation of the first variation, which is well adapted to variational discretization techniques.

Given an initial surface  $\Gamma_0$ , the Willmore flow problem then is to find surfaces  $\Gamma(t)$ , locally parametrized by  $X = X(\cdot, t) : \Omega \rightarrow \Gamma(t)$  for  $t \in [0, T)$  with  $\Gamma(0) = \Gamma_0$  and satisfying the system

$$X_t = -W'(X). \quad (1.3)$$

The system (1.3) is a nonlinear system of  $n+1$  degenerate, strongly coupled parabolic partial differential equations. Starting from the initial value  $X_0$ , which parametrizes the initial surface  $\Gamma_0$ , one has to determine  $X : \Omega \times (0, T) \rightarrow \mathbb{R}^{n+1}$ , such that  $X(\cdot, 0) = X_0$  and

$$X_t + \Delta_{\Gamma}^2 X + \left( 2|\nabla_{\Gamma} \nu|^2 - \frac{1}{2} |\Delta_{\Gamma} X|^2 \right) \Delta_{\Gamma} X = 0.$$

Here  $\nabla_{\Gamma}$  is the tangential gradient on the surface  $\Gamma$ . Note that also  $\Delta_{\Gamma}$  and  $\nabla_{\Gamma}$  are nonlinearly depending on  $X$ .

Information about the geometric properties of the Willmore functional are contained in the book by Willmore [21]. Simonett proved in [20] that a unique local solution of (1.3) exists provided that  $\Gamma_0$  is a compact, closed, immersed and orientable two-dimensional  $C^{2,\alpha}$ -surface in  $\mathbb{R}^3$ . The solution exists globally in time if  $\Gamma_0$  is sufficiently close to a sphere in  $C^{2,\alpha}$ . Using different methods, Kuwert and Schätzle [16] obtained global existence of solutions provided that  $\int_{\Gamma_0} (\kappa_1 - \kappa_2)^2$  is sufficiently small. They were subsequently able to remove the smallness assumption and to prove global existence of a smooth solution of Willmore flow provided that  $W(X_0) \leq 16\pi$ , where  $\Gamma_0 = X_0(S^2)$  (see [17]). Note that our definition differs from the one used in [17] for two-dimensional surfaces by a factor of 2. The numerical evidence of [18] indicates that the above condition is optimal in the sense that the flow develops a singularity if the initial surface has energy greater than  $16\pi$ .

The numerical approach to the parametric Willmore flow problem started with the work [14], in which Brakke's surface evolver was applied to the Willmore functional. In [18] a finite difference scheme was derived to approximate axisymmetric solutions

of Willmore flow. Rusu derived in [19] a variational form which used a mixed method with position and mean curvature vector as independent variables and allowed the use of piecewise linear finite elements for the spatial discretization. This approach was extended in [3] to surfaces with boundaries and applied to problems in surface restoration. A generalization to anisotropic Willmore flow is contained in [6]. A discretization for the parametric Willmore functional, which is based on principles of discrete geometry, is presented in [2].

The computational method depends on the mathematical model which is chosen to represent the surface or interface. In applications all models appear: parametric surfaces, implicit surfaces (level set) and graphs. Let us mention some works on the numerical treatment of the Willmore flow problem using other surface models than the parametric one. In [7] a level set formulation for Willmore flow was derived. The paper [4] contains a convergence proof and error estimates for the Willmore flow of two-dimensional graphs. A variant of the Willmore functional is the Mumford–Shah–Euler functional in image processing [13]. The Willmore functional also plays a decisive role in modelling cell membranes in biology [8] and in materials science.

Willmore flow for curves is normally called elastic flow of curves. There are numerous results concerning the numerical treatment of this problem. We mention [11] and [1].

For a survey of discretization techniques for geometric evolution problems we refer to [5].

The paper is organized as follows. We begin in Sect. 2 with concepts of elementary differential geometry. There we also introduce the concept of the tangential or surface gradient. This concept is essential for our discretization of Willmore flow. It is to the effect that in the end we use tangential gradients of functions defined on polyhedral surfaces. The advantage then is that on each simplex (triangle for  $n = 2$ ) of the discrete surface the tangential gradient is a cartesian (planar) one. Thus the implementation is similar to a planar finite element method. Only the nodes of the triangulation are  $n + 1$ -dimensional instead of  $n$ -dimensional. This method was introduced in [9] for linear elliptic PDEs on surfaces, used in [10] for the computation of mean curvature flow and extended to linear parabolic PDEs on evolving surfaces in [12]. The application of these discretization techniques to the Willmore flow problem is described in Sect. 5. Section 3 provides basic properties of the Willmore functional. Here we calculate the first variation of the functional in a form which is essential for the discretization by finite elements. In Sect. 4 we formulate the Willmore flow problem with the use of the formulas obtained in the previous sections. Then we discretize the Willmore functional with piecewise linear finite elements and prove consistency in Sect. 6. The algorithm for Willmore flow and its stability in natural norms is contained in Sect. 7. We provide numerical tests and examples in Sect. 9, which confirm our theoretical results.

## 2 Notation

Throughout this paper we assume that  $\Gamma \subset \mathbb{R}^{n+1}$  is a smooth, orientable, connected and compact hypersurface without boundary. We assume that  $\Gamma$  is as smooth as will

be needed but at most  $C^{3,1}$ . For numerical purposes we will use the notion of the tangential or surface gradient of a function. See [5, 15] for a more detailed exposition of this material. The tangential gradient of  $f : \Gamma \rightarrow \mathbb{R}$  on the surface  $\Gamma$  with normal  $\nu$  is defined as

$$\nabla_{\Gamma} f = \nabla f - \nabla f \cdot \nu \nu = ((\nabla_{\Gamma})_1 f, \dots, (\nabla_{\Gamma})_{n+1} f). \quad (2.1)$$

Here  $\nabla$  denotes the  $n+1$ -dimensional gradient. The tangential gradient is the projection of the gradient in the ambient space,  $\nabla_{\Gamma} f = P \nabla f$ , with the projection

$$P_{ij} = \delta_{ij} - \nu_i \nu_j \quad (i, j = 1, \dots, n+1). \quad (2.2)$$

The evaluation of the tangential gradient thus requires an extension of  $f$  into a neighbourhood of the surface, which for smooth  $\Gamma$  is easily obtained. The tangential gradient only depends on the values of  $f$  on the surface.

The Laplace–Beltrami-Operator on  $\Gamma$  is defined as the tangential divergence of the tangential gradient:

$$\Delta_{\Gamma} f = \nabla_{\Gamma} \cdot \nabla_{\Gamma} f = \sum_{i=1}^{n+1} (\nabla_{\Gamma})_i (\nabla_{\Gamma})_i f. \quad (2.3)$$

The principal curvatures  $\kappa_i$ , ( $i = 1, \dots, n$ ) of  $\Gamma$  are the nonzero eigenvalues of the symmetric matrix (extended Weingarten map or “shape operator”)

$$\mathcal{H}_{ij} = (\nabla_{\Gamma} \nu)_{ij} = (\nabla_{\Gamma})_i \nu_j \quad (i, j = 1, \dots, n+1). \quad (2.4)$$

Mean curvature then is the trace of this matrix:

$$H = \text{trace } \mathcal{H} = \sum_{i=1}^n \kappa_i.$$

Note that this differs from the more common definition by the factor  $n$ . An important equation which will be used extensively in the algorithms is

$$-\Delta_{\Gamma} \text{id}_{\Gamma} = H \nu, \quad (2.5)$$

where clearly  $\text{id}_{\Gamma}(x) = x$  for  $x \in \Gamma$ . Let us also mention that for the identity map on  $\Gamma$  we have the relation

$$\nabla_{\Gamma} \cdot \nu = \nabla_{\Gamma} \text{id}_{\Gamma} : \nabla_{\Gamma} \nu \quad (2.6)$$

for any smooth function  $\nu$  on  $\Gamma$ .

We recall that the formula for integration by parts on the surface  $\Gamma$  is

$$\int_{\Gamma} \nabla_{\Gamma} f = \int_{\Gamma} f H \nu + \int_{\partial\Gamma} f \mu \tag{2.7}$$

with the conormal vector  $\mu$  on  $\partial\Gamma$ . For closed surfaces the boundary is empty and the last term in (2.7) vanishes. For more details we refer to [5].

Since we want to treat immersions  $\Gamma$  too the notion of tangential gradient has to be understood in a localized sense. At a self intersection of the surface it then is clear from the parametrization which normal has to be chosen for the computation of the tangential gradient.

For later use we write the quantities which we introduced above in a more differential geometric setting. For this we assume that  $\Gamma$  is given locally by some diffeomorphism  $X : \Omega \rightarrow \Gamma \cap U$  with an open set  $U \subset \mathbb{R}^{n+1}$  and some parameter domain  $\Omega \subset \mathbb{R}^n$ . We use the notation  $X = X(\theta)$  with  $\theta \in \Omega$  and introduce the standard notations

$$g_{ij} = X_{\theta_i} \cdot X_{\theta_j}, \quad g = \det(g_{ij}) \quad (i, j = 1, \dots, n) \tag{2.8}$$

for the induced metric and upping of indices denotes the inversion of the matrix:

$$(g^{ij})_{i,j=1,\dots,n} = (g_{ij})_{i,j=1,\dots,n}^{-1}.$$

Then it is easily shown [5], that for functions  $u : \Gamma \rightarrow \mathbb{R}, v : \Gamma \rightarrow \mathbb{R}$  and  $U(\theta) = u(X(\theta)), V(\theta) = v(X(\theta))$  one has

$$(\nabla_{\Gamma} u) \circ X = g^{ij} U_{\theta_j} X_{\theta_i}, \quad ((\nabla_{\Gamma})_r u) \circ X = g^{ij} U_{\theta_j} X_{\theta_i}^r, \tag{2.9}$$

$$(\nabla_{\Gamma} u \cdot \nabla_{\Gamma} v) \circ X = g^{ij} U_{\theta_i} V_{\theta_j}, \tag{2.10}$$

and

$$(\Delta_{\Gamma} u) \circ X = \frac{1}{\sqrt{g}} \left( \sqrt{g} g^{ij} U_{\theta_j} \right)_{\theta_i},$$

where here and in the following we use the convention that we sum over doubly appearing indices.

For  $(n + 1) \times (n + 1)$  matrices  $A$  and  $B$  we denote by  $A : B = \sum_{i,j=1}^{n+1} A_{ij} B_{ij}$  the matrix scalar product. A dot means the euclidean scalar product of vectors:  $a \cdot b = \sum_{i=1}^{n+1} a_i b_i$ .

### 3 The Willmore functional

As mentioned earlier it will be convenient to work with the identity map on the surface  $\Gamma$ . We define  $u : \Gamma \rightarrow \mathbb{R}^{n+1}$  by

$$u(X(\theta)) = \text{id}_{\Gamma}(X(\theta)) = X(\theta), \quad \theta \in \Omega.$$

The Willmore functional is defined as

$$W(u) = \frac{1}{2} \int_{\Gamma} H^2. \quad (3.1)$$

Following the calculations in [21] the first variation of the Willmore functional at  $u$  in the direction of  $\varphi : \Gamma \rightarrow \mathbb{R}^{n+1}$  is given as

$$\langle W'(u), \varphi \rangle = - \int_{\Gamma} \varphi \cdot \nu \left( \Delta_{\Gamma} H - \frac{1}{2} H^3 + H |\mathcal{H}|^2 \right),$$

where  $|\mathcal{H}|^2 = |\nabla_{\Gamma} \nu|^2 = \kappa_1^2 + \dots + \kappa_n^2$ . For two-dimensional surfaces this can be written as

$$\langle W'(u), \varphi \rangle = - \int_{\Gamma} \varphi \cdot \nu \left( \Delta_{\Gamma} H + \frac{1}{2} H^3 - 2HK \right)$$

with Gaussian curvature  $K = \kappa_1 \kappa_2$ . We mention that the term  $HK$  will be a problem for discretization techniques because it is not a divergence term—in contrast to  $H$ .

In the following we derive a form of the first variation of the Willmore functional which is well adapted to discretization techniques using finite elements. Terms like the Gaussian curvature for two-dimensional surfaces or  $|\mathcal{H}|^2$  for  $n$ -dimensional surfaces will not appear in the final formula because we will not use integration by parts on the surface.

For the proofs we shall use the classical differential geometric notation of charts. The notation with tangential gradients then has to be understood up to a partition of unity on the surface  $\Gamma$ .

We start with the first variation of the area functional

$$A(u) = \int_{\Gamma} 1, \quad (3.2)$$

where  $u$  is the identity map on  $\Gamma$ . The formal setting is as follows. We set

$$X_{\epsilon}(\theta) = X(\theta) + \epsilon \Phi(\theta)$$

for  $\theta \in \Omega$ , where  $\Phi : \Omega \rightarrow \mathbb{R}^{n+1}$  is smooth and vanishes near  $\partial\Omega$ . Consequently, we write  $u_{\epsilon}(X_{\epsilon}(\theta)) = X_{\epsilon}(\theta)$  and  $\varphi(X(\theta)) = \Phi(\theta)$ , so that

$$u_{\epsilon} \circ X_{\epsilon} = u \circ X + \epsilon \varphi \circ X \quad \text{on} \quad \Omega.$$

With  $\Gamma_{\epsilon} = X_{\epsilon}(\Omega)$  we then have the following lemma.

**Lemma 1** *The first variation of the area functional at  $u = id_\Gamma$  in the direction of  $\varphi : \Gamma \rightarrow \mathbb{R}^{n+1}$  is given by*

$$\langle A'(u), \varphi \rangle = \frac{d}{d\epsilon} A(u_\epsilon) \Big|_{\epsilon=0} = \int_\Gamma \nabla_\Gamma \cdot \varphi = \int_\Gamma \nabla_\Gamma u : \nabla_\Gamma \varphi. \tag{3.3}$$

*Proof* We define  $g_\epsilon = \det(g_{\epsilon,ij})$  with  $g_{\epsilon,ij} = X_{\epsilon\theta_i} \cdot X_{\epsilon\theta_j}$ . Then the well known Euler relation for the derivative of the determinant gives

$$\frac{\partial}{\partial \epsilon} \sqrt{g_\epsilon} \Big|_{\epsilon=0} = g^{ij} X_{\theta_i} \cdot \Phi_{\theta_j} \sqrt{g} \tag{3.4}$$

and so

$$\begin{aligned} \frac{d}{d\epsilon} A(u_\epsilon) \Big|_{\epsilon=0} &= \frac{d}{d\epsilon} \Big|_{\epsilon=0} \int_\Omega \sqrt{g_\epsilon} \, d\theta = \int_\Omega g^{ij} X_{\theta_i} \cdot \Phi_{\theta_j} \sqrt{g} \, d\theta \\ &= \int_\Gamma \nabla_\Gamma \cdot \varphi = \int_\Gamma \nabla_\Gamma u : \nabla_\Gamma \varphi. \end{aligned}$$

The last two equalities follow from (2.9) and (2.6). □

We calculate the second variation of the area functional in a form which is well adapted to our numerical purposes. Here it is essential that no derivatives of the normal appear, since in our numerical schemes the normal of a discrete polygonal surface will be piecewise constant and discontinuous.

**Lemma 2** *The second variation of the area functional at  $u = id_\Gamma$  in the directions  $\varphi$  and  $\psi$  is given by*

$$\begin{aligned} A''(u)(\varphi, \psi) &= - \int_\Gamma (\nabla_\Gamma)_s \varphi^r (\nabla_\Gamma)_r \psi^s + \int_\Gamma \nu_r \nu_s \nabla_\Gamma \varphi^s \cdot \nabla_\Gamma \psi^r + \int_\Gamma \nabla_\Gamma \cdot \varphi \nabla_\Gamma \cdot \psi. \end{aligned} \tag{3.5}$$

*Proof* Obviously for the second variation at  $u$  in the direction of  $\varphi$  we have from (3.3) with  $\varphi_\epsilon = \varphi \circ X \circ X_\epsilon^{-1}$

$$A''(u)(\varphi, \varphi) = \frac{d}{d\epsilon} \Big|_{\epsilon=0} \int_{\Gamma_\epsilon} \nabla_{\Gamma_\epsilon} \cdot \varphi_\epsilon = \frac{d}{d\epsilon} \Big|_{\epsilon=0} \int_\Omega g_\epsilon^{ij} X_{\epsilon\theta_i} \cdot \Phi_{\theta_j} \sqrt{g_\epsilon} \, d\theta$$

The equation  $g_\epsilon^{ik} g_{\epsilon kj} = \delta_{ij}$  leads to

$$\frac{\partial g_\epsilon^{ij}}{\partial \epsilon} \Big|_{\epsilon=0} = -g^{il} g^{kj} (X_{\theta_k} \cdot \Phi_{\theta_l} + X_{\theta_l} \cdot \Phi_{\theta_k}).$$

We use this equation together with (3.4) and the fact that  $X_\epsilon = X + \epsilon\Phi$  and get

$$\begin{aligned} A''(u)(\varphi, \varphi) &= - \int_{\Omega} g^{il} g^{kj} (X_{\theta_k} \cdot \Phi_{\theta_l} + X_{\theta_l} \cdot \Phi_{\theta_k}) X_{\theta_i} \cdot \Phi_{\theta_j} \sqrt{g} \, d\theta \\ &\quad + \int_{\Omega} g^{ij} \Phi_{\theta_i} \cdot \Phi_{\theta_j} \sqrt{g} \, d\theta + \int_{\Omega} g^{ij} X_{\theta_i} \cdot \Phi_{\theta_j} g^{kl} X_{\theta_k} \cdot \Phi_{\theta_l} \sqrt{g} \, d\theta. \end{aligned} \quad (3.6)$$

We rewrite this equation in terms of tangential gradients. First, by (2.9)

$$g^{ij} X_{\theta_i} \cdot \Phi_{\theta_j} g^{kl} X_{\theta_k} \cdot \Phi_{\theta_l} = ((\nabla_{\Gamma} \cdot \varphi) \circ X)^2. \quad (3.7)$$

Also,

$$\begin{aligned} g^{il} g^{kj} X_{\theta_k} \cdot \Phi_{\theta_l} X_{\theta_i} \cdot \Phi_{\theta_j} &= g^{il} g^{kj} X_{\theta_k}^r \Phi_{\theta_l}^s X_{\theta_i}^r \Phi_{\theta_j}^s = g^{il} X_{\theta_i}^s \Phi_{\theta_l}^r g^{kj} X_{\theta_k}^r \Phi_{\theta_j}^s \\ &= ((\nabla_{\Gamma})_s \varphi^r) \circ X \quad ((\nabla_{\Gamma})_r \varphi^s) \circ X, \end{aligned} \quad (3.8)$$

and finally because of

$$g^{il} X_{\theta_i}^r X_{\theta_l}^s = \delta_{rs} - \nu_r \nu_s$$

we have from (2.10)

$$\begin{aligned} -g^{il} g^{kj} X_{\theta_l} \cdot \Phi_{\theta_k} X_{\theta_i} \cdot \Phi_{\theta_j} + g^{ij} \Phi_{\theta_i} \cdot \Phi_{\theta_j} &= \nu_r \nu_s g^{kj} \Phi_{\theta_k}^s \Phi_{\theta_j}^r \\ &= \nu_r \nu_s (\nabla_{\Gamma} \varphi^s \cdot \nabla_{\Gamma} \varphi^r) \circ X. \end{aligned} \quad (3.9)$$

We now insert the results (3.7), (3.8) and (3.10) into (3.6) and get

$$\begin{aligned} A''(u)(\varphi, \varphi) &= - \int_{\Gamma} (\nabla_{\Gamma})_s \varphi^r (\nabla_{\Gamma})_r \varphi^s + \int_{\Gamma} \nu_r \nu_s \nabla_{\Gamma} \varphi^s \cdot \nabla_{\Gamma} \varphi^r + \int_{\Gamma} (\nabla_{\Gamma} \cdot \varphi)^2. \end{aligned} \quad (3.10)$$

Polarization of the symmetric bilinear form  $A''(u)$  then implies the claim of the lemma.  $\square$

The main idea of our method is to use a weak form of the negative mean curvature vector  $v = \Delta_{\Gamma} u = -H\nu \in L^2(\Gamma)^{n+1}$  with  $u(x) = x$  as second independent variable. We define  $v$  weakly by

$$\int_{\Gamma} v \cdot \psi + \int_{\Gamma} \nabla_{\Gamma} u : \nabla_{\Gamma} \psi = 0 \quad \forall \psi \in H^1(\Gamma)^{n+1}. \quad (3.11)$$

Note that this equation can be understood as defining  $v$  as the  $L^2$ -projection of the functional  $\Delta_\Gamma u$ . Or as

$$(v, \psi)_{L^2(\Gamma)} = -\langle A'(u), \psi \rangle \quad \forall \psi \in H^1(\Gamma)^{n+1}$$

with the area functional  $A$ .

**Lemma 3** *Let  $v$  be the  $L^2(\Gamma)$ -projection of the first variation of area  $A$  according to*

$$\int_\Gamma v \cdot \psi + \int_\Gamma \nabla_\Gamma u : \nabla_\Gamma \psi = 0 \quad \forall \psi \in H^1(\Gamma)^{n+1}. \tag{3.12}$$

*Then the first variation of the Willmore functional at  $u = id_\Gamma$  in the direction of  $\varphi$  is given by*

$$\begin{aligned} \langle W'(u), \varphi \rangle &= -\frac{1}{2} \int_\Gamma |v|^2 \nabla_\Gamma \cdot \varphi - \int_\Gamma \nabla_\Gamma v : \nabla_\Gamma \varphi \\ &\quad - \int_\Gamma \nabla_\Gamma \cdot v \nabla_\Gamma \cdot \varphi + \int_\Gamma D(\varphi) \nabla_\Gamma u : \nabla_\Gamma v, \end{aligned} \tag{3.13}$$

where  $D$  is the symmetric tensor

$$D(\varphi)_{ij} = (\nabla_\Gamma)_i \varphi^j + (\nabla_\Gamma)_j \varphi^i \quad (i, j = 1, \dots, n + 1). \tag{3.14}$$

Here  $\varphi : \Gamma \rightarrow \mathbb{R}^{n+1}$  is an arbitrary variation in space.

Obviously we could replace  $D(\varphi)$  by the matrix  $PD(\varphi)P$ , which maps tangent vectors into tangent vectors, because the last term in (3.13) can be rewritten as

$$D(\varphi) \nabla_\Gamma u : \nabla_\Gamma v = D(\varphi) P \nabla_\Gamma u : P \nabla_\Gamma v = PD(\varphi) P \nabla_\Gamma u : \nabla_\Gamma v.$$

In our calculations  $D$  will always act between tangent spaces and so we will use the definition (3.14).

*Proof* From Lemma 1 we have

$$\begin{aligned} \langle W'(u), \varphi \rangle &= \frac{d}{d\epsilon} W(u_\epsilon) \Big|_{\epsilon=0} = \frac{1}{2} \frac{d}{d\epsilon} \int_{\Gamma_\epsilon} |v_\epsilon|^2 \Big|_{\epsilon=0} \\ &= \int_\Gamma v \cdot \frac{\partial v_\epsilon}{\partial \epsilon} \Big|_{\epsilon=0} + \frac{1}{2} \int_\Gamma |v|^2 \nabla_\Gamma \cdot \varphi, \end{aligned} \tag{3.15}$$

where  $v_\epsilon$  is defined by

$$\int_{\Gamma_\epsilon} v_\epsilon \cdot \psi + \langle A'(u_\epsilon), \psi \rangle = 0 \quad \forall \psi \in H^1(\Gamma_\epsilon)^{n+1}.$$

We differentiate this equation with respect to  $\epsilon$  at  $\epsilon = 0$  using (3.12), Lemmas 1 and 2 and arrive at the relation

$$\int_{\Gamma} \frac{\partial v_{\epsilon}}{\partial \epsilon} \Big|_{\epsilon=0} \cdot \psi + \int_{\Gamma} v \cdot \psi \nabla_{\Gamma} \cdot \varphi + A''(u)(\varphi, \psi) = 0.$$

or

$$\begin{aligned} & \int_{\Gamma} \left( \frac{\partial v_{\epsilon}}{\partial \epsilon} \Big|_{\epsilon=0} \cdot \psi + v \cdot \psi \nabla_{\Gamma} \cdot \varphi \right) \\ &= \int_{\Gamma} \left( (\nabla_{\Gamma})_s \varphi^r (\nabla_{\Gamma})_r \psi^s - \nu_r \nu_s \nabla_{\Gamma} \varphi^s \cdot \nabla_{\Gamma} \psi^r - \nabla_{\Gamma} \cdot \varphi \nabla_{\Gamma} \cdot \psi \right). \end{aligned}$$

We rewrite the term under the second integral in this equation,

$$\begin{aligned} & (\nabla_{\Gamma})_s \varphi^r (\nabla_{\Gamma})_r \psi^s - \nu_r \nu_s \nabla_{\Gamma} \varphi^s \cdot \nabla_{\Gamma} \psi^r \\ &= \left( (\nabla_{\Gamma})_s \varphi^r + (\nabla_{\Gamma})_r \varphi^s \right) (\nabla_{\Gamma})_r \psi^s - \nabla_{\Gamma} \varphi : \nabla_{\Gamma} \psi \\ &\quad - \nu_r \nu_s \left( (\nabla_{\Gamma})_i \varphi^s (\nabla_{\Gamma})_i \psi^r \right) \\ &= D(\varphi)_{si} (\nabla_{\Gamma})_i \psi^s - \nu_r \nu_s D(\varphi)_{is} (\nabla_{\Gamma})_i \psi^r - \nabla_{\Gamma} \varphi : \nabla_{\Gamma} \psi \\ &= D(\varphi)_{si} (\delta_{sr} - \nu_r \nu_s) (\nabla_{\Gamma})_i \psi^r - \nabla_{\Gamma} \varphi : \nabla_{\Gamma} \psi \\ &= D(\varphi)_{is} (\nabla_{\Gamma} u)_{sr} (\nabla_{\Gamma} \psi)_{ir} - \nabla_{\Gamma} \varphi : \nabla_{\Gamma} \psi \\ &= (D(\varphi) \nabla_{\Gamma} u)_{ir} (\nabla_{\Gamma} \psi)_{ir} - \nabla_{\Gamma} \varphi : \nabla_{\Gamma} \psi \\ &= D(\varphi) \nabla_{\Gamma} u : \nabla_{\Gamma} \psi - \nabla_{\Gamma} \varphi : \nabla_{\Gamma} \psi, \end{aligned}$$

where we have used  $\nu_s (\nabla_{\Gamma})_s \varphi^i = \nu \cdot \nabla_{\Gamma} \varphi^i = 0$ , and get

$$\begin{aligned} & \int_{\Gamma} \left( \frac{\partial v_{\epsilon}}{\partial \epsilon} \Big|_{\epsilon=0} \cdot \psi + v \cdot \psi \nabla_{\Gamma} \cdot \varphi \right) \\ & \quad - \int_{\Gamma} \left( D(\varphi) \nabla_{\Gamma} u : \nabla_{\Gamma} \psi - \nabla_{\Gamma} \varphi : \nabla_{\Gamma} \psi - \nabla_{\Gamma} \cdot \varphi \nabla_{\Gamma} \cdot \psi \right) = 0. \end{aligned}$$

Now insert  $\psi = v$  into this equation and deduce the formula

$$\begin{aligned} \int_{\Gamma} \frac{\partial v_{\epsilon}}{\partial \epsilon} \Big|_{\epsilon=0} \cdot v &= - \int_{\Gamma} |v|^2 \nabla_{\Gamma} \cdot \varphi - \int_{\Gamma} \nabla_{\Gamma} \varphi : \nabla_{\Gamma} v - \int_{\Gamma} \nabla_{\Gamma} \cdot v \nabla_{\Gamma} \cdot \varphi \\ & \quad + \int_{\Gamma} D(\varphi) \nabla_{\Gamma} u : \nabla_{\Gamma} v. \end{aligned}$$

We use this equation in (3.15) and have proved formula (3.13).  $\square$

### 4 Willmore flow

Willmore flow is the  $L^2(\Gamma)$ -gradient flow for the Willmore functional. We assume that the evolving surfaces  $\Gamma(t)$  are smooth in space and time and that all the quantities which we shall use make sense. It is convenient to use the topological cylinder

$$G_T = \bigcup_{t \in [0, T]} \Gamma(t) \times \{t\}.$$

Assume that for each  $t \in [0, T]$  the surface  $\Gamma(t)$  is regularly and smoothly parametrized locally by  $X = X(\theta, t)$ ,  $\theta \in \Omega$ . Denote by  $u : G_T \rightarrow \mathbb{R}^{n+1}$  the function

$$u(X(\theta, t), t) = X(\theta, t), \quad \theta \in \Omega, \quad t \in [0, T].$$

For a function  $\eta : G_T \rightarrow \mathbb{R}$  the quantity  $\dot{\eta}$  denotes its material derivative,

$$\dot{\eta} = \eta_t + \mathcal{V} \cdot \nabla \eta, \tag{4.1}$$

where  $\mathcal{V}$  is the velocity of the surface  $\Gamma(t)$  given by

$$\mathcal{V}(X(\theta, t), t) = X_t(\theta, t)$$

and  $\nabla \eta$  is the usual  $(n + 1)$ -dimensional spatial gradient of a smooth extension of  $\eta$  to a neighbourhood of  $G_T$ . Apparently  $\dot{\eta}(X(\cdot, t), t)$  is the time derivative of the function  $\eta(X(\cdot, t), t)$ . Note that (4.1) implies that the material derivative of the identity map  $u(x, t) = \text{id}_{\Gamma(t)}(x) = x$  for  $x \in \Gamma(t)$  is the velocity. We have that

$$\dot{u}(X(\theta, t), t) = (u_t + \mathcal{V} \cdot \nabla u)(X(\theta, t), t)$$

and since  $u_t = 0$  and  $\nabla u(x) = I$  with the unit matrix  $I$  this gives

$$\dot{u}(X(\theta, t), t) = X_t(\theta, t).$$

**Problem 1** (Willmore flow) *For a given surface  $\Gamma_0 \subset \mathbb{R}^{n+1}$  determine a family of smooth surfaces  $(\Gamma(t))_{t \in [0, T]}$  with  $\Gamma(0) = \Gamma_0$ , which move according to the law*

$$\dot{u} = -W'(u),$$

which has to be interpreted as

$$\int_{\Gamma} \dot{u} \cdot \varphi = -\langle W'(u), \varphi \rangle \tag{4.2}$$

for every test function  $\varphi$  and on the time interval  $(0, T]$ .

The Willmore flow problem is a highly nonlinear, degenerate parabolic system of  $n + 1$  PDEs of fourth order. In order to avoid  $C^1$ -elements in a finite element method we write the problem in a mixed form, i.e. we use second order splitting. The results of the previous section and specially Lemma 3 allow the mixed formulation of the Willmore flow problem for  $n$ -dimensional surfaces in a way which is applicable to piecewise linear finite elements.

**Problem 2** For given initial surface  $\Gamma_0$  and  $u_0 = id_{\Gamma_0}$  determine  $u, v : G_T \rightarrow \mathbb{R}^{n+1}$  such that  $u = id_{\Gamma}$ ,  $u(\cdot, 0) = u_0$  on  $\Gamma_0$ , and

$$\begin{aligned} \int_{\Gamma} \dot{u} \cdot \varphi - \int_{\Gamma} \nabla_{\Gamma} v : \nabla_{\Gamma} \varphi + \int_{\Gamma} \nabla_{\Gamma} v : D(\varphi) \nabla_{\Gamma} u \\ - \int_{\Gamma} \nabla_{\Gamma} \cdot v \nabla_{\Gamma} \cdot \varphi - \frac{1}{2} \int_{\Gamma} |v|^2 \nabla_{\Gamma} \cdot \varphi = 0, \end{aligned} \quad (4.3)$$

$$\int_{\Gamma} v \cdot \psi + \int_{\Gamma} \nabla_{\Gamma} u : \nabla_{\Gamma} \psi = 0 \quad (4.4)$$

on the time interval  $(0, T]$  and for all  $\varphi, \psi : G_T \rightarrow \mathbb{R}^{n+1}$ .

## 5 Discretization

The smooth surface  $\Gamma$  is approximated by a polyhedral surface  $\Gamma_h$ . It consists of nondegenerate  $n$ -simplices  $T_h$  in space (triangles for  $n = 2$ )

$$\Gamma_h = \bigcup_{T_h \in \mathcal{T}_h} T_h,$$

which form an admissible triangulation. By  $a_j$  ( $j = 1, \dots, N$ ) we denote the vertices (nodes) of the triangulation. The finite element space is:

$$S_h(t) = \{\eta \in C^0(\Gamma_h(t))^{n+1} \mid \eta|_{T_h} \in \mathbb{P}_1(T_h)^{n+1}, T_h \in \mathcal{T}_h\}.$$

It is spanned by the usual nodal basis  $S_h(t) = \text{span}\{\phi_1, \dots, \phi_N\}^{n+1}$  with  $\phi_i(a_j(t), t) = \delta_{ij}$ . The spatial discretization of Problem 2 now can be written as follows:

**Problem 3** For given initial value  $u_{h0} \in S_h(0)$  determine  $u_h(\cdot, t), v_h(\cdot, t) \in S_h(t)$  such that  $u_h(\cdot, t) = id_{\Gamma_h(t)}$  and

$$\int_{\Gamma_h} \dot{u}_h \cdot \varphi_h - \int_{\Gamma_h} \nabla_{\Gamma_h} v_h : \nabla_{\Gamma_h} \varphi_h + \int_{\Gamma_h} \nabla_{\Gamma_h} v_h : D_h(\varphi_h) \nabla_{\Gamma_h} u_h - \int_{\Gamma_h} \nabla_{\Gamma_h} \cdot v_h \nabla_{\Gamma_h} \cdot \varphi_h - \frac{1}{2} \int_{\Gamma_h} |v_h|^2 \nabla_{\Gamma_h} \cdot \varphi_h = 0 \tag{5.1}$$

$$\int_{\Gamma_h} v_h \cdot \psi_h + \int_{\Gamma_h} \nabla_{\Gamma_h} u_h : \nabla_{\Gamma_h} \psi_h = 0 \tag{5.2}$$

for all  $\varphi_h, \psi_h \in S_h(t)$  and for  $t \in (0, T]$ .

Note that now

$$D_h(\varphi_h)_{ij} = (\nabla_{\Gamma_h})_i \varphi_h^j + (\nabla_{\Gamma_h})_j \varphi_h^i \quad (i, j = 1, \dots, n + 1)$$

and the dot stands for the material derivative with respect to the piecewise linear velocity  $\mathcal{V}_h(x, t) = \sum_{j=1}^N \dot{a}_j(t) \phi_j(x, t)$  of the discrete surface.

### 6 Consistency

In this section we prove that the Willmore functional (3.1) is consistently approximated with piecewise linear finite elements. It is well known that the mean curvature vector itself is not approximated. Nevertheless the use of an adequate Ritz projection will lead to consistency.

We assume that  $\Gamma \in C^{3,1}$  is a hypersurface as in Sect. 2. Let  $\Gamma_h$  be a piecewise linear approximation of  $\Gamma$  which represents an admissible triangulation as in Sect. 5 with vertices sitting on the smooth surface  $\Gamma$ . We also assume that  $h$  is the maximal diameter of a simplex  $T_h \in \mathcal{T}_h$  and that the inner radii of the simplices are bounded from below by  $ch$  with some positive constant  $c$ . The smoothness of  $\Gamma$  implies that there exists a strip

$$U_\delta = \{x \in \mathbb{R}^{n+1} \mid |d(x)| < \delta\}$$

around  $\Gamma$  such that each  $x \in U_\delta$  can be written as

$$x = a(x) + d(x)v(a(x))$$

with the oriented distance function  $d$  of  $\Gamma$  and  $a(x) \in \Gamma$ .

We assume that the triangulation  $\mathcal{T}_h$  is such that  $\Gamma_h \subset U_\delta$  and for each point  $a \in \Gamma$  there is at most one point  $x \in \Gamma_h$  with  $a = a(x)$ . This assumption excludes a possible double covering of the smooth surface  $\Gamma$  by the discrete surface  $\Gamma_h$  and implies that  $a : \Gamma_h \rightarrow \Gamma$  is a bijective map. For an example see Fig. 1 in [12].

For a function  $z$  defined on the discrete surface  $\Gamma_h$  we define its lift  $z^l$  onto the continuous surface  $\Gamma$  by

$$z^l(a(x)) = z(x), \quad x \in \Gamma_h.$$

The inverse process is denoted by  $(z^l)^{-1} = z$ . The lift of the finite element space

$$S_h = \{\eta \in C^0(\Gamma_h)^{n+1} \mid \eta|_{T_h} \in \mathbb{P}_1(T_h)^{n+1}, T_h \in \mathcal{T}_h\}$$

will be denoted by

$$S_h^l = \{\eta^l \mid \eta \in S_h\}.$$

For later use note that the approximation of the geometry of a given smooth surface  $\Gamma$  by the discrete surface was studied in [9, 12]. The following lemma lists the approximation properties of the discrete surface  $\Gamma_h$ . For a proof we refer to [9, Sect. 5], see also [12, Lemma 5.1].

**Lemma 4** *Assume that  $\Gamma$  and  $\Gamma_h$  are as above. Then for the distance between continuous and discrete surface we have the estimate*

$$\|d\|_{L^\infty(\Gamma_h)} \leq ch^2. \quad (6.1)$$

The quotient  $\delta_h$  between the smooth and discrete surface measures  $dA$  and  $dA_h$ , defined by  $\delta_h dA_h = dA$ , satisfies

$$\sup_{\Gamma_h} |1 - \delta_h| \leq ch^2. \quad (6.2)$$

Let  $P$  be as in (2.2) with the discrete analogue  $P_{h,ij} = \delta_{ij} - v_{h,i}v_{h,j}$ , and  $\mathcal{H}$  as in (2.4). Then for the matrix  $R_h = \frac{1}{\delta_h} P(I - d\mathcal{H})P_h(I - d\mathcal{H})$  we have the estimate

$$\sup_{\Gamma_h} |(I - R_h)P| \leq ch^2. \quad (6.3)$$

Note that the gradients between smooth and discrete surface are related by

$$\nabla_{\Gamma_h} z = P_h(I - d\mathcal{H})\nabla_{\Gamma} z^l(a)$$

for a function  $z$  which is defined on the discrete surface  $\Gamma_h$ . The previous lemma then implies that the  $L^2$ - and  $H^1$ -norms on the discrete and continuous surfaces are comparable. In order to prove a consistency result for the Willmore functional we shall need a suitable interpolation. The following lemma is taken from Lemma 5 in [9] for  $n = 2$ . The generalization to  $n = 3$  is easily obtained.

**Lemma 5** Assume that  $\Gamma$  and  $\Gamma_h$  are as above and  $n \leq 3$ . Then for given  $z \in H^2(\Gamma)$  there is an  $I_h z \in S_h^l$  such that

$$\|z - I_h z\|_{L^2(\Gamma)} + h \|\nabla_\Gamma(z - I_h z)\|_{L^2(\Gamma)} \leq ch^2 \|z\|_{H^2(\Gamma)}. \tag{6.4}$$

We are now in a position to prove the consistency of our discretization. We will use a Ritz projection for the definition of the discrete Willmore energy. Theoretically we could choose  $u_h \in S_h$  for given discrete surface  $\Gamma_h$  as the solution of

$$\int_{\Gamma_h} \nabla_{\Gamma_h} u_h : \nabla_{\Gamma_h} \psi_h = \int_{\Gamma} \nabla_\Gamma u : \nabla_\Gamma \psi_h^l \quad \forall \psi_h \in S_h, \quad \int_{\Gamma_h} u_h = \int_{\Gamma} u,$$

where  $u(x) = x$  for  $x \in \Gamma$ . But then we would have to compute integrals over the smooth surface  $\Gamma$ . In the next theorem we will introduce a projection which is more useful in practice. For the projection (6.5) we will only need to compute the projection of barycenters of the simplices  $T_h \subset \Gamma_h$  onto the smooth surface, if we use a modest integration formula. This is easily done numerically.

**Theorem 4** For a given smooth,  $n$ -dimensional ( $n \leq 3$ ) surface  $\Gamma \in C^{3,1}$  let  $u = id_\Gamma$ . Let  $\Gamma_h$  be a corresponding discrete surface as above. Let  $u_h \in S_h$  be the solution of

$$\int_{\Gamma_h} \nabla_{\Gamma_h} u_h : \nabla_{\Gamma_h} \psi_h = \int_{\Gamma_h} \nabla_{\Gamma_h} u^{-l} : \nabla_{\Gamma_h} \psi_h, \quad \int_{\Gamma_h} u_h = \int_{\Gamma_h} u^{-l}. \tag{6.5}$$

for all  $\psi_h \in S_h$ . Then for  $v_h$  defined by (5.2) and  $h \leq h_0$  we have the estimate

$$\|v - v_h^l\|_{L^2(\Gamma)} \leq ch, \tag{6.6}$$

and for the discrete Willmore functional

$$W(u_h) = \frac{1}{2} \int_{\Gamma_h} |v_h|^2$$

we obtain the estimate

$$|W(u) - W(u_h)| \leq ch^2.$$

The constants  $c$  depend on  $\|v\|_{H^2(\Gamma)}$  and on the fourth derivatives of the parametrization of the surface  $\Gamma$ .

*Proof* For arbitrary  $\psi_h \in S_h$  we have by definition that

$$\int_{\Gamma} v \cdot \psi_h^l = - \int_{\Gamma} \nabla_\Gamma u : \nabla_\Gamma \psi_h^l. \tag{6.7}$$

Again by definition together with (6.5) one obtains

$$\int_{\Gamma_h} v_h \cdot \psi_h = - \int_{\Gamma_h} \nabla_{\Gamma_h} u_h : \nabla_{\Gamma_h} \psi_h = - \int_{\Gamma_h} \nabla_{\Gamma_h} u^{-l} : \nabla_{\Gamma_h} \psi_h. \quad (6.8)$$

The difference of continuous and discrete curvature vector then can be estimated as follows:

$$\begin{aligned} \int_{\Gamma} (v - v_h^l) \cdot \psi_h^l &= \int_{\Gamma} v \cdot \psi_h^l - \int_{\Gamma_h} v_h \cdot \psi_h \delta_h \\ &= - \int_{\Gamma} \nabla_{\Gamma} u : \nabla_{\Gamma} \psi_h^l + \int_{\Gamma_h} \nabla_{\Gamma_h} u^{-l} : \nabla_{\Gamma_h} \psi_h + \int_{\Gamma_h} v_h \cdot \psi_h (1 - \delta_h) \\ &= - \int_{\Gamma} \nabla_{\Gamma} u : \nabla_{\Gamma} \psi_h^l + \int_{\Gamma} R_h^l \nabla_{\Gamma} u : \nabla_{\Gamma} \psi_h^l + \int_{\Gamma_h} v_h \cdot \psi_h (1 - \delta_h) \\ &= - \int_{\Gamma} (I - R_h^l) \nabla_{\Gamma} u : \nabla_{\Gamma} \psi_h^l + \int_{\Gamma_h} v_h \cdot \psi_h (1 - \delta_h) \\ &\leq ch^2 \int_{\Gamma} |\nabla_{\Gamma} \psi_h^l| + ch^2 \int_{\Gamma_h} |v_h| |\psi_h|. \end{aligned}$$

This implies that for every  $\psi_h \in S_h$  we have

$$\int_{\Gamma} (v - v_h^l) \cdot \psi_h^l \leq ch^2 \int_{\Gamma} |\nabla_{\Gamma} \psi_h^l| + ch^2 \int_{\Gamma} |v_h^l| |\psi_h^l|. \quad (6.9)$$

And from this estimate we deduce an  $L^2$ -bound for the difference between  $v$  and  $v_h^l$ . The splitting

$$\int_{\Gamma} |v - v_h^l|^2 = \int_{\Gamma} (v - v_h^l) \cdot (v - I_h v) + \int_{\Gamma} (v - v_h^l) \cdot (I_h v - v_h^l)$$

allows us to use (6.9) and with an inverse estimate together with the interpolation estimates from Lemma 5 we get

$$\begin{aligned} \|v - v_h^l\|_{L^2(\Gamma)}^2 &\leq \|v - v_h^l\|_{L^2(\Gamma)} \|v - I_h v\|_{L^2(\Gamma)} \\ &\quad + ch^2 \|\nabla_{\Gamma} (I_h v - v_h^l)\|_{L^1(\Gamma)} + ch^2 \|v_h^l\|_{L^2(\Gamma)} \|I_h v - v_h^l\|_{L^2(\Gamma)} \\ &\leq \|v - v_h^l\|_{L^2(\Gamma)} \|v - I_h v\|_{L^2(\Gamma)} + ch \|I_h v - v_h^l\|_{L^2(\Gamma)} \\ &\quad + ch^2 \left( \|v - v_h^l\|_{L^2(\Gamma)} + \|v\|_{L^2(\Gamma)} \right) \\ &\quad \times \left( \|v - I_h v\|_{L^2(\Gamma)} + \|v - v_h^l\|_{L^2(\Gamma)} \right) \end{aligned}$$

$$\begin{aligned} &\leq ch(1 + \|v\|_{H^2(\Gamma)}) \|v - v_h^l\|_{L^2(\Gamma)} + ch^2 \|v - v_h^l\|_{L^2(\Gamma)}^2 \\ &\quad + ch^4 \|v\|_{L^2(\Gamma)}(1 + \|v\|_{H^2(\Gamma)}) + ch^3 \|v\|_{H^2(\Gamma)}. \end{aligned}$$

For  $h \leq h_0$  we then have the estimate

$$\|v - v_h^l\|_{L^2(\Gamma)} \leq ch(1 + \|v\|_{H^2(\Gamma)}). \tag{6.10}$$

The consistency estimate for the Willmore functional now follows easily. By (5.2) and (3.11) we have

$$\begin{aligned} 2|W(u) - W(u_h)| &= \left| \int_{\Gamma} |v|^2 - \int_{\Gamma_h} |v_h|^2 \right| = \left| \int_{\Gamma} |v|^2 - \int_{\Gamma} |v_h^l|^2 \frac{1}{\delta_h} \right| \\ &\leq \int_{\Gamma} \left| |v|^2 - |v_h^l|^2 \right| + \int_{\Gamma} |v_h^l|^2 \left| 1 - \frac{1}{\delta_h} \right| \\ &\leq \left| \int_{\Gamma} (I_h v + v_h^l) \cdot (v - v_h^l) \right| + \int_{\Gamma} |v - I_h v| |v - v_h^l| + ch^2 \int_{\Gamma} |v_h^l|^2. \end{aligned}$$

With (6.9) we can continue this estimate as

$$\begin{aligned} &\leq ch^2 \left( \|\nabla_{\Gamma} I_h v\|_{L^1(\Gamma)} + \|\nabla_{\Gamma} v_h^l\|_{L^1(\Gamma)} + \|I_h v\|_{L^2(\Gamma)}^2 + \|v_h^l\|_{L^2(\Gamma)}^2 \right) \\ &\quad + \|v - v_h^l\|_{L^2(\Gamma)} \|v - I_h v\|_{L^2(\Gamma)}. \end{aligned}$$

Standard estimates using (6.10), Lemma 5 and inverse inequalities then finally lead to

$$|W(u) - W(u_h)| \leq ch^2 \left( 1 + \|v\|_{H^2(\Gamma)}^2 \right) \tag{6.11}$$

and the theorem is proved. □

### 7 Stability

The derivation of the algorithm in Problem 3 guarantees the stability of the spatially discrete scheme. The norms in which we formulate the stability result are the natural norms for Willmore flow. In the continuous setting this estimate is obtained directly from (4.2). If we choose  $\varphi = \dot{u}$  there, then we obtain

$$\int_{\Gamma(t)} |\dot{u}(\cdot, t)|^2 + \frac{d}{dt} W(u(\cdot, t)) = \int_{\Gamma(t)} |\dot{u}(\cdot, t)|^2 + \langle W'(u(\cdot, t)), \dot{u}(\cdot, t) \rangle = 0$$

for all  $t \in (0, T]$ .

**Theorem 5** Assume that  $u_h, v_h$  is a solution of Problem 3. with initial value  $u_h(\cdot, 0) = u_{h0}$  and set  $\Gamma_{h0} = \Gamma_h(0)$ . Then the energy relation

$$\int_{\Gamma_h} |\dot{u}_h|^2 + \frac{1}{2} \frac{d}{dt} \int_{\Gamma_h} |v_h|^2 = 0$$

holds for all times in  $(0, T]$ . If we choose the discrete initial data  $u_{h0} \in S_h(0)$  in such a way that an estimate of the form

$$\sup_{\varphi_h \in S_h(0)} \|\varphi_h\|_{L^2(\Gamma_{h0})}^{-1} \int_{\Gamma_{h0}} \nabla_{\Gamma_{h0}} u_{h0} : \nabla_{\Gamma_{h0}} \varphi_h \leq c \|u_0\|_{H^2(\Gamma_0)} \quad (7.1)$$

holds, then we have stability of the scheme in adequate norms:

$$\int_0^T \|\dot{u}_h\|_{L^2(\Gamma_h)}^2 dt + \sup_{(0,T)} \|v_h\|_{L^2(\Gamma)}^2 \leq c \|u_0\|_{H^2(\Gamma_0)}^2. \quad (7.2)$$

Condition (7.1) can be satisfied by choosing the discrete initial data as an appropriate Ritz projection of the continuous initial data  $u_0$ . For an example of such a choice we refer to (6.5).

*Proof* The proof follows directly from the consistent derivation of the algorithm. Let us shortly repeat the formal arguments. Equation (5.1) is equivalent to

$$(\dot{u}_h, \varphi_h)_{L^2(\Gamma_h)} + \langle W'(u_h), \varphi_h \rangle = 0. \quad (7.3)$$

also in the spatially discrete setting. In deriving (5.1) in the continuous setting we did not perform any integration by parts and we did not use that the continuous curvature vector  $v$  has normal direction. Thus Lemma 3 also holds for the spatially discrete problem. And just as in that lemma the second variable  $v_h$  is defined by (5.2). We insert  $\varphi_h = \dot{u}_h$  into (7.3) and get

$$\|\dot{u}_h\|_{L^2(\Gamma_h)}^2 + \langle W'(u_h), \dot{u}_h \rangle = 0 \quad (7.4)$$

and thus

$$\|\dot{u}_h\|_{L^2(\Gamma_h)}^2 + \frac{d}{dt} W(u_h) = 0. \quad (7.5)$$

Note that  $\dot{u}_h$  is an admissible test function because by definition one has  $u_h = \text{id}_{\Gamma_h}$  and  $\dot{u}_h(X_h(\theta, t), t) = X_{ht}(\theta, t)$ . Here  $W(u_h)$  has to be interpreted as

$$W(u_h) = \frac{1}{2} \|v_h\|_{L^2(\Gamma_h)}^2$$

for  $v_h$  given by (5.2). This was the first claim of the stability lemma. The second claim is obtained by integrating (7.5) with respect to time:

$$\int_0^t \|\dot{u}_h\|_{L^2(\Gamma_h)}^2 dt + \frac{1}{2} \|v_h(\cdot, t)\|_{L^2(\Gamma_h)}^2 = \frac{1}{2} \|v_h(\cdot, 0)\|_{L^2(\Gamma_{h0})}^2. \tag{7.6}$$

The norm of  $v_h$  at time  $t = 0$  then can be estimated by using (5.2) together with assumption (7.1):

$$\begin{aligned} \|v_h(\cdot, 0)\|_{L^2(\Gamma_{h0})}^2 &= - \int_{\Gamma_{h0}} \nabla_{\Gamma_{h0}} u_{h0} : \nabla_{\Gamma_{h0}} v_h(\cdot, 0) \\ &\leq c \|u_0\|_{H^2(\Gamma_0)} \|v_h(\cdot, 0)\|_{L^2(\Gamma_{h0})}. \end{aligned}$$

We insert this estimate into (7.6) and have proved the estimate (7.2). □

### 8 Time discretization

In contrast to the spatial discretization we do not have analytical results on the stability of our time discretization.

We use the notation  $v^m = v(\cdot, m\tau)$  for the discrete time levels with time step size  $\tau > 0$  and  $m = 1, \dots, M_\tau$  where  $M_\tau \tau = T$ . The discrete spaces are denoted by

$$S_h^m = S_h(m\tau) = \text{span}\{\phi_1^m, \dots, \phi_N^m\}$$

with the nodal basis functions  $\phi_j^m = \phi_j(\cdot, m\tau)$  which were introduced in Sect. 5.

The time discretization is used to linearize the problem in each time step. The idea for this is to take the geometric quantities from the previous time step as this was done in several works about geometric PDEs. See for example [5] for a survey and [10] for a time discretization of mean curvature flow.

**Algorithm 6** (Discrete Willmore flow) *For given initial surface  $\Gamma_h^0$  and  $u_{h0}(x) = x$  for  $x \in \Gamma_h^0$  determine for  $m = 0, \dots, M_\tau - 1$  solutions  $(u_h^{m+1}, v_h^{m+1}) \in S_h^m \times S_h^m$  such that,*

$$\begin{aligned} &\frac{1}{\tau} \int_{\Gamma_h^m} u_h^{m+1} \cdot \varphi_h - \int_{\Gamma_h^m} \nabla_{\Gamma_h^m} v_h^{m+1} : \nabla_{\Gamma_h^m} \varphi_h \\ &+ \int_{\Gamma_h^m} \nabla_{\Gamma_h^m} v_h^{m+1} : D_h(\varphi_h) \nabla_{\Gamma_h^m} u_h^m - \int_{\Gamma_h^m} \nabla_{\Gamma_h^m} \cdot v_h^{m+1} \nabla_{\Gamma_h^m} \cdot \varphi_h \\ &- \frac{1}{2} \int_{\Gamma_h^m} |v_h^m|^2 \nabla_{\Gamma_h^m} u_h^{m+1} : \nabla_{\Gamma_h^m} \varphi_h = \frac{1}{\tau} \int_{\Gamma_h^m} u_h^m \cdot \varphi_h \end{aligned} \tag{8.1}$$

$$\int_{\Gamma_h^m} v_h^{m+1} \cdot \psi_h + \int_{\Gamma_h^m} \nabla_{\Gamma_h^m} u_h^{m+1} : \nabla_{\Gamma_h^m} \psi_h = 0 \quad (8.2)$$

for all  $\varphi_h, \psi_h \in S_h^m$  and set

$$\Gamma_h^{m+1} = u_h^{m+1}(\Gamma_h^m).$$

For this algorithm a trick was used to make the scheme more implicit. Because in the continuous problem one has  $\nabla_{\Gamma} \cdot \varphi = \nabla_{\Gamma} u : \nabla_{\Gamma} \varphi$ , the term  $|v_h|^2 \nabla_{\Gamma_h} \cdot \varphi_h$  was discretized with respect to time as  $|v_h^m|^2 \nabla_{\Gamma_h^m} u_h^{m+1} : \nabla_{\Gamma_h^m} \varphi_h$ .

Let us look at the matrix-vector form of the algorithm. For each  $m$  we define the following matrices:

$$\begin{aligned} M_{kl} &= \int_{\Gamma_h^m} \phi_k^m \phi_l^m, & S_{kl} &= \int_{\Gamma_h^m} \nabla_{\Gamma_h^m} \phi_k^m \cdot \nabla_{\Gamma_h^m} \phi_l^m, \\ Q_{kl} &= \frac{1}{2} \int_{\Gamma_h^m} |v_h^m|^2 \nabla_{\Gamma_h^m} \phi_k^m \cdot \nabla_{\Gamma_h^m} \phi_l^m \end{aligned} \quad (8.3)$$

and

$$\begin{aligned} (S^{rs})_{kl} &= S_{kl}^{rs} = \int_{\Gamma_h^m} (\nabla_{\Gamma_h^m})_r \phi_k^m (\nabla_{\Gamma_h^m})_s \phi_l^m, \\ (R^{rs})_{kl} &= R_{kl}^{rs} = \int_{\Gamma_h^m} (\delta_{rs} - v_r^m v_s^m) \nabla_{\Gamma_h^m} \phi_k^m \cdot \nabla_{\Gamma_h^m} \phi_l^m \end{aligned} \quad (8.4)$$

for  $k, l = 1, \dots, N$  and  $r, s = 1, \dots, n+1$ . Here  $v^m$  is the unit normal to  $\Gamma_h^m$ .  $M$  is the mass matrix and  $S$  is the stiffness matrix on the  $m$ th time level. Note that all these matrices can be computed with elementary integration formulas. Here and in the following we suppress the dependency of matrices and vectors on  $m$ . The basis functions  $\phi_j^m$  depend on  $m$  too, since we are working with an evolving basis.

The solution  $(u_h^{m+1}, v_h^{m+1})$  can be expressed as

$$u_h^{m+1}(x) = \sum_{j=1}^N u_j \phi_j^m(x), \quad v_h^{m+1}(x) = \sum_{j=1}^N v_j \phi_j^m(x), \quad x \in \Gamma_h^m$$

with coefficients  $u_j, v_j \in \mathbb{R}^{n+1}$ . We form the jets  $u, v \in \mathbb{R}^{N(n+1)}$ ,

$$\begin{aligned} u &= (u_1, \dots, u_N) = \left( (u_1^1, \dots, u_1^{n+1}), \dots, (u_N^1, \dots, u_N^{n+1}) \right), \\ v &= (v_1, \dots, v_N) = \left( (v_1^1, \dots, v_1^{n+1}), \dots, (v_N^1, \dots, v_N^{n+1}) \right), \end{aligned}$$

and use the notations

$$u^r = (u_1^r, \dots, u_N^r), \quad v^r = (v_1^r, \dots, v_N^r) \quad (r = 1, \dots, n + 1).$$

Then the matrix-vector form of Algorithm 6 is given by the following algorithm:

**Algorithm 7** For each time step  $m = 0, \dots, M_\tau - 1$  compute the matrices according to (8.3), (8.4) and solve with right hand side

$$b_k^r = \frac{1}{\tau} \int_{\Gamma_h^m} x_r \phi_k^m(x) dA(x) \quad (k = 1, \dots, N)$$

the linear system

$$\frac{1}{\tau} M u^r - S v^r + \sum_{s=1}^{n+1} R^{sr} v^s + \sum_{s=1}^{n+1} (S^{sr} - S^{rs}) v^s - Q u^r = b^r, \quad (8.5)$$

$$M v^r + S u^r = 0 \quad (8.6)$$

for  $r = 1, \dots, n + 1$ .

This linear system of equations is solved by a Schur complement approach and the BICG algorithm.

As we want the algorithm to be applicable to immersed surfaces too, we mention that the neighbourhood relations between the simplices of  $\Gamma_h$  in the finite element program guarantee that self intersections do not affect the algorithm. See [5] for the evolution of an unstable Willmore sphere with self intersections.

## 9 Numerical results

### 9.1 Consistency tests

We start with consistency tests for the Willmore functional. For this we approximate the continuous surface  $\Gamma$  by an interpolation (possibly use a grid smoothing algorithm) and then calculate the Ritz type projection from Theorem 4.

For quantities  $E(h_1)$  and  $E(h_2)$  which are calculated for the grid sizes  $h_1$  and  $h_2$  the experimental order of convergence is defined as

$$\text{eoc}(h_1, h_2) = \log \frac{E(h_1)}{E(h_2)} \left( \log \frac{h_1}{h_2} \right)^{-1}.$$

*Example 1* The unit sphere  $\Gamma = S^2$ —in fact any two-dimensional sphere—has Willmore energy  $8\pi$ . We approximate  $\Gamma$  by discrete spheres  $\Gamma_h$  and calculate their discrete Willmore energies  $W(u_h) = \frac{1}{2} \int_{\Gamma_h} |v_h|^2$  with  $v_h$  given by (5.2). As a macro triangulation we used an octahedron. In Table 1 we show the maximal diameter  $h$

**Table 1** Approximation of the Willmore energy  $W(u) = 8\pi \approx 25.1327$  of the unit sphere  $S^2$ 

$N$	$h$	$W(u_h)$	$W(u) - W(u_h)$	eoc	$W(\tilde{u}_h)$	$W(u) - W(\tilde{u}_h)$
34	0.707106	14.685165	10.447570	–	21.064188	0.161882
130	0.513578	21.843107	3.289628	3.61	25.022492	0.00438645
514	0.280935	24.248481	0.884255	2.18	26.140487	–0.0400971
2,050	0.143613	24.906125	0.226610	2.03	26.428208	–0.0515452
8,194	0.0722037	25.075551	0.0571843	2.00	26.501071	–0.0544443
32,770	0.0361516	25.118388	0.0143478	2.00	26.519625	–1.386889

Columns 3–5 show the approximation results with the use of the Ritz procedure in Theorem 4: second order approximation. Columns 6,7 show the results without using a Ritz procedure: no consistency

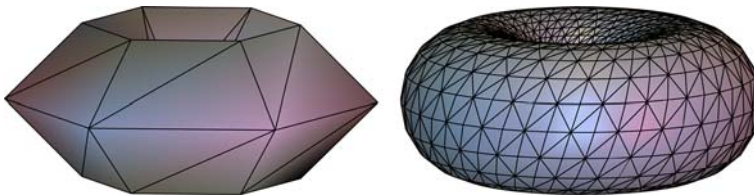


**Fig. 1** Triangulations of the Clifford torus (9.1). *Left* macro triangulation, *right* smoothed grid after three refinements

of a triangle on  $\Gamma_h$ , the discrete Willmore energy and the error between the continuous and discrete energies together with an eoc. Apparently, the Willmore energy is approximated quadratically for piecewise linear elements as it was stated in Theorem 4. Two columns of Table 1 show the results for the computation of the Willmore energy without using a Ritz type projection. Here we chose  $\tilde{u}_h = id_{\Gamma_h}$ . We see that in this case we do not have consistency of the discretization.

*Example 2* As a second test for consistency we calculate the discrete Willmore energy of a Clifford torus

$$\Gamma = \left\{ x \in \mathbb{R}^3 \mid \left( 1 - \sqrt{x_1^2 + x_2^2} \right)^2 + x_3^2 = \frac{1}{2} \right\}. \quad (9.1)$$

In Fig. 1 we show the macro triangulation and the discrete surface after three refinements. The final grid is obtained as follows: we start with the macro triangulation and refine it successively. In each refinement step we project the new nodes vertically onto the smooth surface. We then smooth this grid with a Laplace method, where we move each node into the center of the neighbouring nodes—projected onto the smooth surface. This is the initial discrete surface  $\tilde{\Gamma}_h$  for the computation of the Willmore energy. We then calculate a Ritz type projection  $u_h$  as introduced in (6.5) of  $u = id_{\Gamma}$ . We calculate  $v_h$  from (5.2) and calculate the Willmore energy with the help of this function. The result of this consistency test is shown in Table 2.

**Table 2** Approximation of the Willmore energy  $W(u) = 4\pi^2 \approx 39.4784$  of the Clifford torus (9.1)

$N$	$h$	$W(u_h)$	$W(u) - W(u_h)$	eoc
192	0.883663	35.312635	4.165765	–
768	0.445644	37.250387	2.228014	0.91
3,072	0.224260	38.893089	0.585312	1.95
12,288	0.127597	39.332252	0.146149	2.46
49,152	0.0739198	39.440890	0.0375110	2.49

### 9.2 Examples

We did not use any grid smoothing algorithm for the subsequent computations.

*Example 3* Spheres are minima of the Willmore functional with Willmore energy  $8\pi$ . In Fig. 2 we show the evolution of a deformed sphere into a round sphere. The value of the Willmore energy during the evolution is plotted in Fig. 3 together with the grid regularity parameter

$$\sigma = \max_{T \in \mathcal{T}_h} \frac{h(T)}{\rho(T)}.$$

Here  $h(T)$  is the diameter of the triangle  $T$  and  $\rho(T)$  denotes the radius of the inner circle of the triangle.

*Example 4* In Fig. 4 we show how a thin torus evolves to a Clifford torus. The initial torus has larger radius 1.0 and smaller radius 0.2. We used a grid with 1536 nodes with  $h = 0.265360$ . The final value of the Willmore functional at time 0.02434 was  $W = 38.142639$ .

*Example 5* In Fig. 5 we show how a strongly perturbed Clifford torus evolves to the Clifford torus.

*Example 6* The Willmore functional for two-dimensional surfaces is invariant under conformal transformations in  $\mathbb{R}^3$ . These transformations are given by similarity transformations and point inversions (see [21]). In Fig. 6 we show an inverted Clifford torus which represents a minimum of the (discrete) Willmore functional. This surface was computed with our evolutionary algorithm. The initial surface was obtained by the point inversion

$$F(x) = x_0 - 4 \frac{x - x_0}{|x - x_0|^2}, \quad x_0 = (2, 0, 0).$$

The stationary solution to which the surface evolves is  $F(\Gamma)$ , where  $\Gamma$  is the Clifford torus given by (9.1). The discrete Willmore energy was 46.4864.

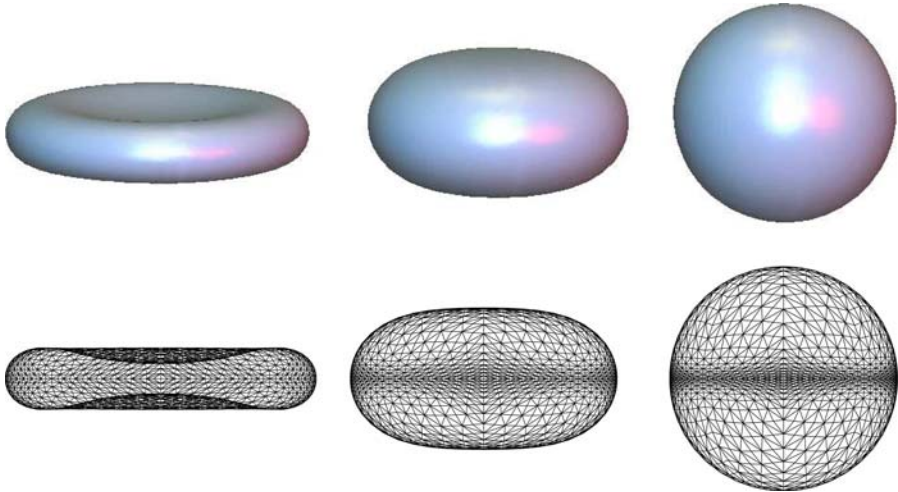


**Fig. 2** Willmore flow towards a sphere. We show the surface at times  $t = 0.001755$ ,  $t = 0.01053$  and  $t = 0.04387$  (upper row). The second row shows the grid at the same times

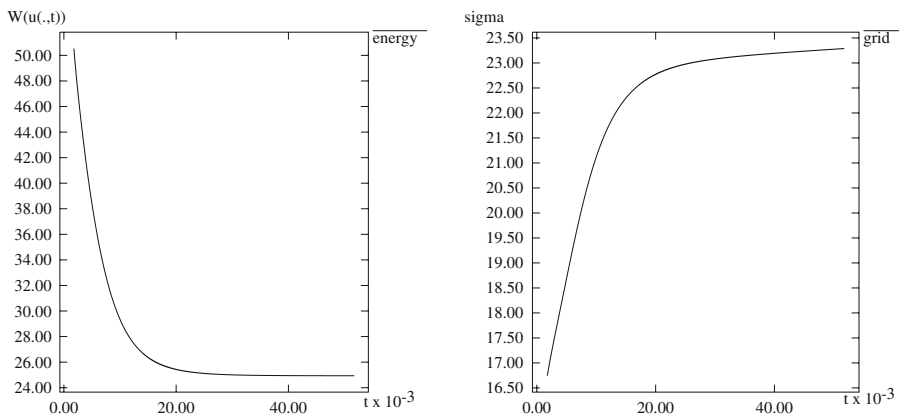


**Fig. 3** Values for the Willmore energy against time (left) and values of the grid parameter  $\sigma$  against time (right) for the computation shown in Fig. 2



**Fig. 4** Willmore flow of a thin torus towards a Clifford torus (cut open). The times  $t = 0.0$ ,  $t = 10^{-5}$ ,  $t = 2 \times 10^{-5}$  and  $t = 2.5 \times 10^{-5}$  are shown

We finish with an example for the Willmore flow of a surface of genus two. For this we glue together two tori as is shown in Fig. 7. There we show some time steps of the evolution. The grid contained 3433 nodes and the time step varied between  $10^{-7}$  in the beginning and  $10^{-4}$  in the end. We stopped the calculations when the solution

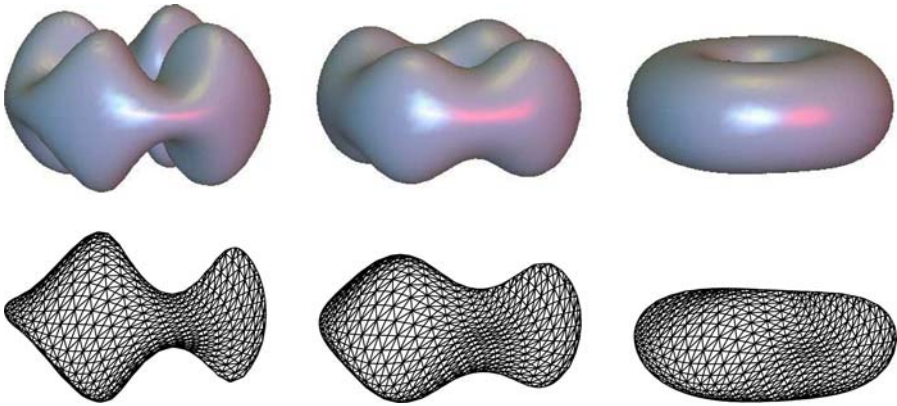


**Fig. 5** Willmore flow of a strongly deformed torus towards a Clifford torus. *Second row* part of the computational surface grid outside the ball with center  $(0, 1, 0)$  and radius 2.25

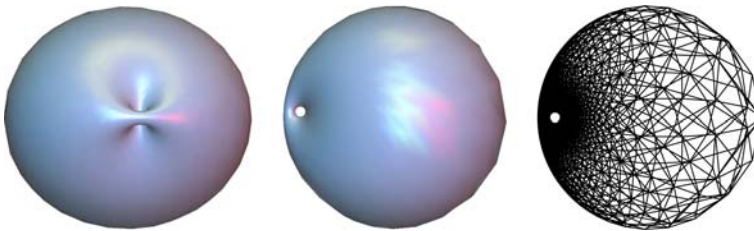


**Fig. 6** A minimum of the discrete Willmore functional: inverted Clifford torus. The surface is shown from the  $x_1$ -axis (*left*) and the  $x_3$ -axis (*middle and right*)

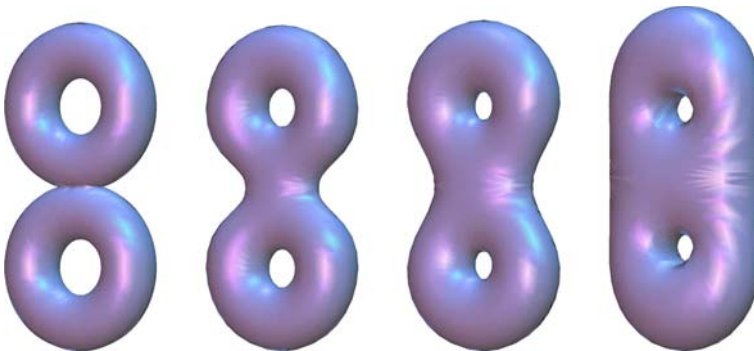


**Fig. 7** Evolution of a double torus under Willmore flow for the times  $t = 0.0$ ,  $t = 0.01477$ ,  $t = 0.03321$  and  $t = 0.1531$

apparently became stationary in the sense that the value of the Willmore functional changed for less than  $10^{-4}$  between two time steps. The final value of the functional was 49.7674 at time 0.1599526.

**Acknowledgments** This work was supported by the Deutsche Forschungsgemeinschaft via the Forschergruppe 469 “Nonlinear partial differential equations: Theoretical and numerical analysis.” We thank Ernst Kuwert for many helpful and interesting discussions. And we thank Claus-Justus Heine for providing a macro triangulation for the double torus. The graphical representations were done with the programs GRAPE and xgraph.

## References

1. Barrett, J.W., Garcke, H., Nürnberg, R.: A parametric finite element method for fourth order geometric evolution equations. *J. Comp. Phys.* **222**, 441–467 (2007)
2. Bobenko, A., Schroeder, P.: Discrete Willmore flow, SIGGRAPH '05: ACM SIGGRAPH 2005 (Courses). ACM Press, New York (2005)
3. Clarenz, U., Diewald, U., Dziuk, G., Rumpf, M., Rusu, R.: A finite element method for surface restoration with smooth boundary conditions. *Comput. Aided Geometr. Des.* **21**, 427–445 (2004)
4. Deckelnick, K., Dziuk, G.: Error analysis for the Willmore flow of graphs. *Interfaces Free Boundaries* **8**, 21–46 (2006)
5. Deckelnick, K., Dziuk, G., Elliott, C.M.: Computation of geometric partial differential equations and mean curvature flow. *Acta Numer.* 139–232 (2005)
6. Diewald, U.: Anisotrope Krümmungsflüsse parametrischer Flächen sowie deren Anwendung in der Flächenverarbeitung, Dissertation University Duisburg-Essen (2005)
7. Droske, M., Rumpf, M.: A level set formulation for Willmore flow. *Interfaces Free Boundaries* **6**, 361–378 (2004)
8. Du, Q., Liu, C., Wang, X.: Simulating the deformation of vesicle membranes under elastic bending energy in three dimensions. *J. Comp. Phys.* **212**, 757–777 (2006)
9. Dziuk, G.: Finite elements for the Beltrami operator on arbitrary surfaces. *Partial Differ. Equ. Calculus Var. Lect. Notes Math.* **1357**, 142–155 (1988)
10. Dziuk, G.: An algorithm for evolutionary surfaces. *Numer. Math.* **58**, 603–611 (1991)
11. Dziuk, G., Kuwert, E., Schätzle, R.: Evolution of elastic curves in  $\mathbb{R}^n$ : existence and computation. *SIAM J. Math. Anal.* **33**, 1228–1245 (2002)
12. Dziuk, G., Elliott, C.M.: Finite elements on evolving surfaces. *IMA J. Numer. Anal.* **27**, 262–292 (2006)
13. Feng, X., Prohl, A.: Analysis of gradient flow of a regularized Mumford–Shah functional for image segmentation and image inpainting. *Math. Model. Numer. Anal.* **38**, 291–320 (2004)
14. Francis, G., Sullivan, J.M., Kusner, R.B., Brakke, K.A., Hartman, C., Chappell, G.: The minimax sphere eversion. In: Hege, H.-C., Polthier, K. (eds) *Visualization and Mathematics*, pp. 3–20. Springer, Heidelberg (1997)
15. Gilbarg, D., Trudinger, N.S.: *Elliptic partial differential equations of second order*. Grundlehren der mathematischen Wissenschaften, Springer, Heidelberg (1998)
16. Kuwert, E., Schätzle, R.: The Willmore flow with small initial energy. *J. Differ. Geom.* **57**, 409–441 (2001)
17. Kuwert, E., Schätzle, R.: Removability of point singularities of Willmore surfaces. *Ann. Math.* **159**, 1–43 (2004)
18. Mayer, U.F., Simonett, G.: A numerical scheme for axisymmetric solutions of curvature-driven free boundary problems, with applications to the Willmore flow. *Interfaces Free Boundaries* **4**, 89–109 (2002)
19. Rusu, R.: An algorithm for the elastic flow of surfaces. *Interfaces Free Boundaries* **7**, 229–239 (2005)
20. Simonett, G.: The Willmore flow near spheres. *Differ. Integral Equ.* **14**, 1005–1014 (2005)
21. Willmore, T.J.: *Riemannian Geometry*. Oxford (1993)